STUDIES ON IRRADIATION EFFECTS OF SILICON-ON-SAPPHIRE DEVICES AND PROTON BEAM DIVERGENCE THROUGH PRINTED CIRCUIT BOARDS

Approved by:

Dr. Jingbo Ye

Prof. Ryszard Stroynowski

Prof. Robert Kehoe

STUDIES ON IRRADIATION EFFECTS OF SILICON-ON-SAPPHIRE DEVICES AND PROTON BEAM DIVERGENCE THROUGH PRINTED CIRCUIT BOARDS

A thesis Presented to the Graduate Faculty of the

Dedman College

Southern Methodist University

in

Partial Fulfillment of the Requirements

for the degree of

Master of Science

with a

Major in Physics

by

John Norton P

(B.S., Baylor University, 2006)

July 31, 2008

Norton P, John B.S., Baylor University, 2006

Studies on Irradiation Effects of Silicon-On-Sapphire Devices and
Proton Beam Divergence through Printed Circuit Boards

Advisor: Professor Jingbo Ye

Master of Science degree conferred July 31, 2008

thesis completed July 31, 2008

A series of Geant4 based Monte Carlo simulations are used to explore and understand various radiation induced effects in semiconductor devices and environments. Beam quality and stray radiation of protons through FR4 printed circuit boards is studied to better understand beam conditions in a proton irradiation test environment involving many stacked printed circuit boards. Attention is payed to Silicon on Sapphire semiconductors and their behavior in the presence of radiation. A study of deposited energy versus beam incidence angle is done to extend experimental measurements irradiation at multiple incidence angle, and to better understand possible causes for digital signal bit-flip. Finally, the effects of an electric field on the charge distribution in sapphire in the presence of a cobalt-60 source are simulated.

FIX ME GODDAMN

TABLE OF CONTENTS

LIST OF FIGURES

LIST OF TABLES

Table Page

This dissertation is dedicated to me graduating

Chapter 1

INTRODUCTION

1.1. Motivation

1.1.1. ATLAS

The ATLAS detector offers a window into the new particle physics phenomena offered by the Large Hadron Collider (LHC), located at the European Center for Nuclear Research (CERN). The detector contains precision instruments like the liquid argon calorimeter, used to measure the energies of created particles. These contain a multitude of fast electronics used to record and process a substantial amount of data while maintaining the pace of 40Mhz frequency of collisions. High luminosity of the accelerator coupled with crucial timing requires that readout electronics be able to cope for years with incoming signals. In addition, the locations of readout electronics are inaccessible and premature replacement is out of the question. For this purpose, a method for qualifying and testing electronics components has ben accepted by the ATLAS collaboration. Tests conducted at Southern Methodist University(SMU) are briefly explained here and subsequently presented in full. Focus is then paid to questions raised by the tests, and Monte Carlo simulations are offered as an attempt to clarify the uncertainty raised by these experiments. Shown in figure 1.1 is a cutaway of the ATLAS detector.

1.1.2. Radiation Tolerant Electronics Procurement

Electronics components used near the detector are bombarded by predominantly secondary particles coming from interactions with primary particles and detector materials. This means that particle energies crossing electrical components are less than a few GeV, and have high flux and homogeneous directions [3]. The dominant radiation types include, but are not limited to, photons and electrons at levels of 5Gy/yr and charged hadrons at fluxes in excess of $7.7 \times 10^{10}\ cm^{-2}yr^{-1}$ for energies greater than 20 MeV [3].

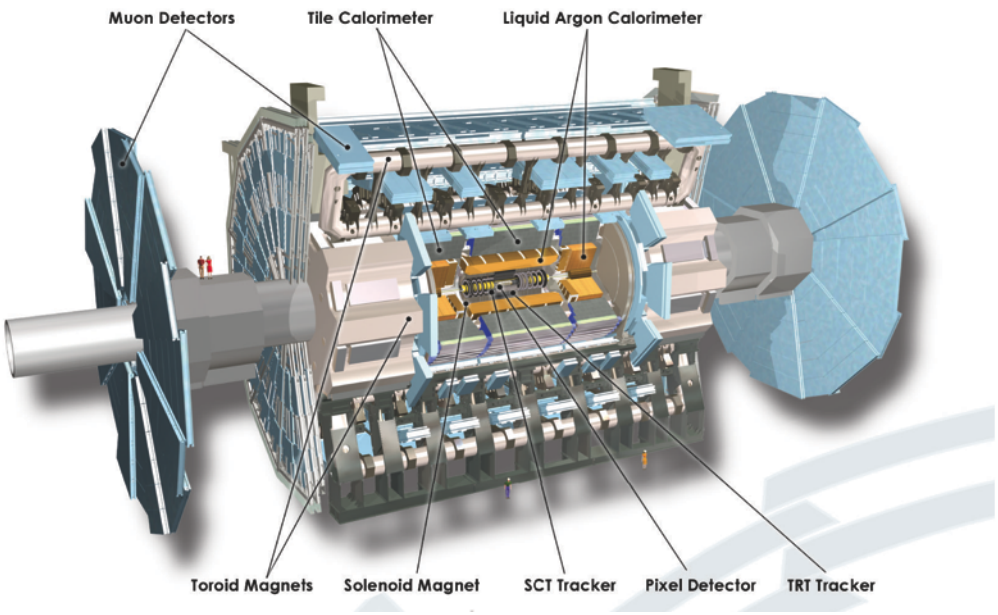

Figure 1.1. ATLAS Detector Cutaway

Due to high requirements and stringent testing, there are two sources for such capable electronics. These are application specific integrated circuits (ASICs) and components off the shelf (COTS) [3]. The radiation tolerance level of ASICs is ideally guaranteed by the manufacturer and is developed to certain specifications. Nevertheless, ASIC samples are still tested in order to identify defective lots. Once a prototype is tested according to ATLAS specifications and is deemed adequate, entire lots of such ASICs are purchased, knowing that they all are guaranteed to perform accordingly. In a COTS model, pre-selected generic components, that satisfy the design requirements of the electronics are tested according to ATLAS specifications. If the high radiation behavior of pre-selected COTS is adequate, then lots of from which the initial samples came, are purchased for future uses. In this way, the responsibility of radiation robustness lies in the tester as the vendor only provides samples of existing products. Either way, physical tests are done extensively to predict or fine-tune the behavior of potential electronics under the high radiation environment of the ATLAS detector and it's surrounding cavern.

1.1.3. Radiation Tolerance Specifications

Table 1.1. Simulated Radiation Levels, Liquid Argonne Calorimeter[5]

$System$	$position(cm)$				SRL_{tid}	SRL_{see}
	$Zmin$	$Zmax$	$Rmin$	$Rmax$	$Gy \times 10yr^{-1}$	$hadrons \times cm^{-2}10yr^{-1}$
$LAr, barrel$	300.0	350.0	290.0	340.0	$4.87E+01$	$7.67E+11$
$LAr, endcap$	620.0	670.0	290.0	340.0	$5.67E+00$	$2.14E+10$

The specifications of the doses electronics must endure is related to the simulated radiation level (SRL) for each particular region of the ATLAS detector. The liquid argon calorimeter (LAr) will be the main focus throughout the cited examples. Table 1.1 lists the reported simulated radiation levels for the LAr[5].

1.1.4. Radiation Tolerance Testing Methods

The ATLAS procedure for electronics testing is a modified method based on the department of defense MIL STD 883 test method 1017.2 and the ESA SCC basic specification no. 22900 [3]. The ATLAS standard for total ionization dose (TID) effects testing, which examines the effects of cumulative energy deposition in the oxide layer of electronic components, is based upon gamma-ray and X-ray exposures. When looking for single event effects (SEE's) the ATLAS standard procedure is to expose the device to a beam of protons and to watch for various forms of SEE's [3].

1.1.5. Tests Performed by SMU

SMU performed several tests using a silicon on sapphire (SOS) device. These included TID tests wherein a single device is irradiated using a Cobalt-60 source, a test of the sapphire substrate resistivity under similar conditions, and a search for single event upsets (SEU's) using the device irradiated by a beam of 230 MeV protons. Shown in figure 1.2 is the test apparatus used to measure the devices performance under irradiation from a Cobalt-60 source. Although results are obtained, as will be seen in the next section, a few uncertainties are left to which clarification from Monte Carlo simulation is attempted.

1.2. SEMICONDUCTOR TESTS

Figure 1.2. Irradiation Setup

As a contribution to the planned upgrade to the ATLAS detector, SMU tested a silicon on sapphire device (SOS) manufactured by semiconductor manufacturer for it's behavior under radiation environments similar to what it would see near the ATLAS detector of the Super-LHC. The most important aspects to cover in the testing are: total ionizing dose (TID) behavior, and single event upsets (SEUs). The former is characterized, in this experiement, by an increase in leakage current in the two types of devices that compose the microchip under the prolonged exposure of gamma-rays. Leakage current is defined by current flow between the source and drain of a transistor which is operating below it's threshold voltage. The threshold voltage is the voltage needed to be applied to the gate in order for at least a linear relationship between gate voltage and source-drain current. SEUs are searched for by irradiating the microchip while it processes data input. The way this is done is to input data on a string of shift registers, and compare the output to the expected output. An SEU will manifest itself as a single bit being flipped and consequently, incorrect output. Finally, a test of the resistivity of the sapphire substrate layer is done while under the influence of gamma-rays as in the TID test. The consequences of a sudden drop in resistivity of the sapphire substrate layer would be an increase in the possibility for induced electric fields between the source and drain of what is essentially a collection of field effect transistors (FETs). This would cause an increase in leakage current.

1.2.1. Semiconductor Irradiation, TID

In this experiment, the SOS device is irradiated using a Co-60 source in an effort to measure the leakage current in what is known as the back channel[6]. In other words, the leakage current induced by the potential difference between the sapphire substrate and the device layer. Among other reasons, the main idea behind the sapphire layer being suspect is one of size, as the sapphire layer is 200 microns while the adjacent layer is on the order of 100 nanometers[6]. The SOS device in question consists of both n-type and p-type MOSFET devices and the affects of the Co-60 source are measured independently as they will behave quite differently under such circumstances. It is suggested that leakage current in NMOS transistors is caused by radiation induced "holes" in large quantities at the silicon-device interface, while leakage current in PMOS transistors is caused by an excess of electrons at the sapphire-device interface. Because these two phenomena compete against each-other, the end result is a polarity change of the sapphire substrate during irradiation. As such, NMOS transistors experience a rise in leakage current when the dose is low, followed by a decrease of

leakage current as the dose increases, and PMOS transistors experience almost no change until high dose situations[6]. In either case, it is in fact electron-hole pairs that are produced, with either the electron or hole "migrating" away or recombining near the sapphire-device interface, thus causing a pile-up of the remaining partner. It is this electron distribution that will be simulated in Geant4 under various circumstances mimicking the actual experiment, the likes of which will be explained in the coming paragraphs. A brief look at the results will better motivate the choice and structure of the Geant4 simulations. These are gone into detail in chapter 3 and briefly below. A curious finding manifests itself when the sapphire substrate is grounded. Upon grounding the sapphire layer, no noticeable increase in leakage currents in either NMOS or PMOS transistors are measured. To better understand this phenomenon, electric potentials other than simply a ground are applied to better understand the mechanism by which charge pile-up is reduced. Knowing the voltage applied (+30V and -30V) to the bottom of the sapphire substrate, a Geant4 program with the corresponding electric field inside the sapphire can be used to plot the theoretical electron distributions in sapphire after it is irradiated with 1.2 MeV photons.

1.2.2. Semiconductor Irradiation, SEU

Using the same setup, a 230 MeV proton beam is shot at the device in order to measure single event upsets (SEU's) in the shift registers of the device. For this particular experiment, no errors where reported before, after, or during the irradiation period[6]. There is, however, the question of how this beam of protons behaves during the test. The proton beam not only has to travel through the relatively small SOS devices, it has to travel through all of the supporting equipment including an array of printed circuit boards covered in copper etching. Measuring the migration of the proton beam from it's original configuration as it passes through said PCBs is yet another simple setup easily handled by a Geant4 simulation.

1.2.3. Resistivity Measurement

Further experimentation is done to passively measure the resistivity of the sapphire bulk used in Silicon-on-Sapphire devices. The test setup consists of 9 SOS chips in parallel wherein an electric potential of 30 volts is applied, and a pico-ammeter to measure the current draw of the chips. The resistivity is the given by $p = V/I * A/L$ where A is the cross-sectional area of the chip, and L is the path length along which the resistivity is measured. In this case, $L = 0.02cm$ and $A = 0.81cm^2$.

Sapphire normally has a resistivity greater than $1e14 ohm/cm$ and as such a very small current will be measured[7]. It was found that, during irradiation, the 9 sapphire blocks indeed changed resistivity as evident by a positive current being measured. This is in contrast to the very small negative current measured before and after the irradiation.

1.3. Geant4

Large scale high energy physics experiments, such as ATLAS and the LHC, are always on a very grand scale. This will only continue to grow. In the more than a decade long development of such a detector as ATLAS, the "measure twice, cut once" moniker comes into play using simulation after simulation of what certain detector designs can be expected to do. This lies at the heart of the motivation for a standardized, reliable means for such simulations. This is why Geant currently exists. As will be shown, Geant4's structure strives to be one of flexibility and extensibility. It has a long history with the high energy physics field, from which it derives much of its utility and direction.

Geant4 is a toolkit for the simulation of the passage of particles through matter [4]. It is a large C++ toolkit that allows one to write a simulation program taking full advantage of Monte Carlo based routines for experimentally verified particle physics. With a very simple core design, Geant4 simply iterates through any particle's trajectory, noting the surrounding material and choosing subsequent steps based on user included physics processes. Based on these processes, the parent particle may undergo any number of processes including those that may produce child particles. As Geant4 is just a toolkit, it is up to the program developer to decide what the above processes output. The simplest case is the output of tracking data (particle coordinates, energy, etc...) in plain ASCII text via standard output, and a more complex case being the direct filling of ROOT ntuples and histograms. In order to output any useful information various classes and routines in Geant4 must be queried for current tracking information. Once this is done, the options are limitless, as the application is being written in industry standard C++.

1.3.1. Geant4 History

In 1993, two independent sources, CERN and KEK, began investigating possible improvements for the FOTRAN based Geant3 simulation software. In 1994 this was formally proposed under proposition RD44 and submitted to CERN's research and development committee. The initial

motivation was to create a detector simulation toolkit to simulate next generation particle physics experiments. The possible market for such a tool in other fields, such as medical and space physics, however, motivated the project to extend it's scope beyond that of high energy particle physics. The goal was to use the latest ideas in object oriented programming to achieve an intuitive application layer that provides a consistent means for future growth (i.e. new physics processes). Today, Geant4 is around 30 megabytes of source code and over 75 megabytes of data tables for a large variety of physical processes.

1.3.2. Geant4 Structure

Geant4 takes full advantage of the concept known as object oriented programming. Geant4 is, at heart, simply a large collection of C++ classes containing pertinent routines and complex data types. Much of Geant4 is derived from a relatively small subset of base classes.

This set of base classes is best described using what are simply called "Geant4 Categories." These are as follows: Run, Event, Tracking, Physics Processes, Hits and Digitization, Geometry, Electromagnetic Fields, Materials, Global Usage, Visualization, and Intercoms.

1.3.2.1. Geometry

Central to the way geometry is specified in Geant4 are the concepts of a physical volume and a logical volume. A logical volume is a detector element, possibly containing other volumes, which has associated with it all the specifics and information not having anything to do with physical placement. A physical volume is the physical location and orientation of a detector element (in most cases, the respective logical volume).

1.3.2.2. Materials

Materials defined in Geant4 are either of class G4Element or G4Material. There are a large number of predefined materials in Geant4, ranging from compounds such as carbon dioxide, to materials such as blood and bone. Any material can be built using G4Elements and other materials, by specifying fractional content and density.

1.3.2.3. Electromagnetic Fields

Although not a well documented section in the Geant4 manual, field definitions are quite simple in Geant4. They exist as a modification that is attached to volumes via a FieldManager class. Fields

can also be attached to the experimental world as a whole.

1.3.2.4. Particles

All particles are defined through the G4Particle class. Information contained in each particle's class ranges from charge and mass, to decay properties in the case of particles such as muons and pions.

1.3.2.5. Physics Processes

All Geant4 physics processes conform to the G4VProcess interface and are separated into 3 sub-categories. The first is the decay sub-category. This process gets the step length from the mean lifetime of the particle. Upon decay, the particle is queried for decay products and their branching ratios. The second sub-category is that of electromagnetic processes. This is a collection of processes divided into sections as follows: standard, low energy, muons, x-rays, optical, and stills. These are self explanatory save for the stills and standard sections, which provide basic operations for electrons, positrons, photons, and charged hadrons, and utility classes used by all electromagnetic processes respectively. The final category of physics processes is that of hadronic physics. The hadronic physics classes provide an interface to the various modeling techniques for hadronic physics. Most of these models are very specific in their usefulness, and cover a wide array of approximation techniques and energy regimes. There is a "standard" model used that satisfies the most general use-case for hadronic shower simulations.

1.3.2.6. Run

The Run category contains the master classes used to manage collections of events that share common beam and geometry parameters. In an actual program this category is manifest, traditionally, as the first and last major events of the main function. A Geant4 program starts by constructing a G4RunManager class, and ends by deleting the one (and only) G4RunManager object[**?**].

1.3.2.7. Event

The Event category consists of classes used to process single events. Usage of the term "event" in this context is as in high energy physics, wherein an event is a snapshot of an interaction and it's decay products, either simulated or measured in a detector. In Geant4, this means an event consists of particle generation (or the calling of an external particle generator in some cases), parent

and child particle tracking, detector reaction, and everything in-between. Obviously certain simple Geant4 based applications (such as the ones discussed in the subsequent pages) do not simulate detector reaction (for example the simulated detector readout system of particles passing through a calorimeter) however, the same nomenclature is used within the Geant4 program in order to keep uniformity with other Geant4 programs[**?**].

1.3.2.8. Tracking

Arguably the most important category, Tracking does just that. A look into this category is best motivated using the pertinent classes. The key classes for tracking in Geant4 are G4TrackingManager and G4SteppingManager. G4TrackingManager keeps all information related to the particles track, as well as tabulating actions necessary to complete a track. The tracking class then pushes the particle by a step size determined dynamically, based on the active processes and what they mandate. Throughout this step, the G4SteppingManager class maintains information concerning the particular step[**?**].

1.3.2.9. Hits and Digitization

In a large scale colider-detector, it is important not only to simulate the known physical processes, but also how the detector will respond to such events. The means for this is separated into two classes of attributes and routines, hits, and digits. In a Geant4 simulation, in order for a detector's response to be modeled, sensitive detectors need to be defined. These are volumes in which each particle interaction and child particles are tracked, and output. Non-sensitive detectors simply report energy deposition and modify a particles trajectory accordingly. A Sensitive detector is used to define areas of the detector that matter for the purpose of collecting data, whereas non-sensitive detectors exist to react accordingly to incoming particles, but data from these interactions is either not wanted, or otherwise useless in the scheme of the experiment. A digit is defined as output for a single hit in a single volume, interpreted as if it goes through all of the physical instrumental readout and processing. This could be the digital pulse a wire chamber would give after processing, given an ionization track. It is important to note that in the following simulations, no sensitive detectors are defined, and as a result, all volumes and all interactions report full tracking information, which is then processed externally.

1.3.2.10. Communication

The rest of the Geant4 categories relate to control and communication of running simulations. This includes user interfaces such as a shell-like environment and visualizations of events and geometry such as opengl. The main interactive interpreter is tcsh, which is a commonly used, modern shell.

1.3.3. Geant4 Uses

Geant4 has spawned some widely used projects including the ATLAS detector simulation. Some smaller projects are the Mulassis project which aims to provide a simple means to measure cosmic radiation dose rates on pertinent devices and the GATE project which is used in medical physics to simulate tomographic emission scanners.

1.4. Monte Carlo Projects

The Geant4 simulations written and described here are the result of unanswered questions, stemming from a study done by SMU wherein a semiconductor irradiation study was performed in order to benchmark the response of a Silicon-On-Sapphire semiconductor device in the presence of high radiation. The three experiments carried out by SMU described in the previous sections raised a few questions that will attempt to be clarified using several Geant4 based simulations. These include a study of proton beam divergence as the beam passes through printed circuit boards (PCBs), a study of single event effects and device orientation, and a look at the effects of an electric field imposed in the sapphire substrate on the distribution of free electrons induced by TID radiation.

1.4.1. Incident Beam Divergence

The first exercise in a trio of Geant4 simulations is a study of printed circuit boards(PCB's) in the presence of a fairly stout proton beam. The main motivation is to assess both the beam dispersion as it passes through the PCB's and the stray radiation that is scattered at extreme angles, resulting in what can be described as contamination of the surrounding environment (in this case, the room containing the PCB's and other sensitive equipment). This exercise is pertinent to situations where first tier readout electronics must be placed near the beam or possible collision areas. The proton-pcb simulation consists of 10, equally spaced, PCB's covered by a thin film of copper. The copper is to roughly simulate the presence of the complex circuit connections, which are usually traces of copper on the surface of the circuit board. The material chosen for the PCB's is the industry standard FR4 circuit board material which is composed of glass fiber and epoxy. A $230MeV$ proton beam with a uniform distribution within a circular spot will be shot incident to the row of PCB's, and the evolution of the beam's shape will be tracked as the beam passes through the PCB's. Stray radiation will be monitored using particles which leave the experiment world through planes parallel to the beam line, and an estimate of ambient dosage will be assessed.

1.4.2. Silicon on Sapphire

In a high radiation environment, a clear choice for radiation hard microprocessors is the Silicon-On-Sapphire (SOS) device. This is known to have very robust characteristics under high radiation. The two major means by which a complex semiconductor is affected by radiation are an electric field between the source and drain of single or multiple devices caused by charge buildup near the device

or a single event upset caused by a heavy ionizing particle passing through a single device, causing a sudden cascading flow of charge. The first simple simulation is to probe possible causes and scenerios for single event upsets. This is done by using heavy ionizing particles, such as protons, in an energy regime that mimics the aforementioned physical experiment. A small, preliminary monte carlo is run in order to predict the energy deposition of $230MeV$ in the whole device (both silicon and sapphire layers). This means a block consisting of a $200micron$ sapphire layer and a $100nm$ silicon layer. The particles have normal incidence on the silicon face as this is how the experiment is setup. The incidence is then changed in an order to look for a noticeable increase or decrease in total energy deposition. This is done as an investigation as to whether the aforementioned experiments might have missed something (the experiment is only done with normal incidence). Data is gathered for normal, 0, 30, and 60 degree incidence angles. The same setup is also run with the sapphire end facing the beam. This is also done in order to see if the silicon layer experiences more interaction behind the sapphire layer as opposed to in front of it.

1.4.3. Irradiated Sapphire

Concerning the former of the two causes for semiconductor missbehavior, attention will be placed on charge distribution in the bulk of the device as a result of irradiation. One of the main concerns that is left is that of free electrons inside the material as a result of bombardment and subsequent dominant processes like Compton scattering. This study looks to assess, through a Geant4 simulation, the migration of free electrons caused solely by radiation bombardment. The main area of study is a situation in which a $200micron$ sapphire block is placed in the presence of a cobalt-60 source. This mandates a beam of $1.2MeV$ photons.

This situation is further augmented by a look into the effects of a forced electric field throughout the sapphire. This is done as a possible active solution for minimizing the distribution of free electrons in the sapphire. Also, the presence of the electric field can skew the free electron distribution thus biasing the electrons to one side of the sapphire block. This is significant as such biasing could force electrons that are "knocked" free to "even out" presumably filling positively charged "holes" that although not simulated, must be there as free electrons come from ionized lattice sites in the sapphire crystal. If one could tune the bias in order to match the initial ionization distribution with the distribution of free electrons after migration (down to the final low energy interaction that causes Geant4 to stop tracking), it is conceivable that the possibility of induced unwanted currents

near or in the silicon layer could be minimized, and with it the negative effects of a high radiation environment.

1.4.4. Tools

Tools used in the above simulations include Geant4 version 9.1[**?**], the ROOT object oriented framework version 5.16[2] and the text processing tools grep, sed, and awk. Grep, sed, and awk are used to filter the output of all Geant4 programs used, as ascii text was chosen as the output of choice given the author's experience in text manipulation. ROOT was used to create histograms and otherwise analyze the data and fill binary ntuples to reduce the disk space used. All Geant4 programs that where used for final data production where written from scratch, using the guidance of the many Geant4 example programs. In the last incarnation of simulations, a master framework was used, that has the ability to simulate all situations needed. An XML geometry file is created with parameters such as geometry and material definitions, which exists outside of the program itself (thus not needing to be re-compiled). This XML file follows the syntax defined by GDML or "Geometry Description Markup Language" developed as an extension to Geant4 at CERN[1]. See the appendix for code and further description.

Chapter 2

PHYSICAL EXPERIMENT DETAIL

2.1. The Device

As a possible replacement to components used in the optical readout boards of the ATLAS detector (details...), $0.25 micrometer$ silicon-on-sapphire devices where purchased from a commercial semiconductor company in order to test their radiation tolerance. The device is a Silicon-on-Sapphire Complimentary Metal-Oxide Semiconductor (CMOS), using a $100nm$ silicon layer on top of a $200micron$ sapphire substrate. The Silicon on Insulator family of semiconductors is especially desirable for it's radiation tolerance. This is by in large attributed to the artificially grown sapphire crystals whose high resistivity helps mitigate the effects of stray charges caused by radiation. Since the device is a large collection of metal-oxide-semiconductor field effect transistors, or MOSFETs, each of which is either a p-type, or n-type MOSFET (NMOS and PMOS), the dialogue used in subsequent analysis and introspection is as if a single MOSFET is focused on, rather than the entire, complex, device.

2.2. Irradiated SOS device, TID

In order to measure the effects of a total ionizing dose (TID) on the SOS device in question, a cobalt-60 source was used to irradiate the device at a dose rate of 1.2kRad/hr. Programmable DC powersupplies where used to supply several NMOS and PMOS devices with a voltage of 2.5 volts between the drain and source (V_{DS}) for NMOS and -2.5 volts for the V_{DS} of the PMOS devices. The voltage between the gate and source (V_{GS}) was set to 0 for both NMOS and PMOS devices. A picoammeter was used to measure current flow between the drain and source of all devices[6]. Before and after the irradiation, the current flow is measured as it responds to an applied V_{GS} between 0.0 and 1.5 volts for NMOS and -1.5 and 0.0 volts for PMOS devices. Shown in 2.1 is the result of such measurements before and after 33kRad and 86kRad total dose runs. It can be seen from the figure 2.1 that for NMOS devices threshold voltage (that is, the voltage at which the I-V curve is linear)

decreases, while leakage current (the current flow before threshold voltage is reached) increases with a 33kRad dose. For the same NMOS devices, a 86kRad dose yields an increase in threshold voltage and leakage current stays the same as before the irradiation[6]. For PMOS devices, it is shown in figure 2.1 that the threshold voltage and leakage current stay unchanged after a dose of 33kRad. After a dose of 86kRad, however, the threshold voltage absolute value decreases, while the leakage current increases[6]. A second set of runs was done with the sapphire substrate grounded. Threshold voltages and leakage current in NMOS and PMOS devices are measured throughout the irradiation as shown in figure 2.2. As can be seen from figure 2.2, threshold voltage and leakage current changes are negligible throughout the course of the irradiation.

2.2.1. Conclusions

An increase in leakage current can be attributed to several phenomena, all of which involve trapped charge accumulations in various portions of the device. These trapped charges can either be in the gate oxide, the field oxide, or the sapphire substrate. The gate oxide is the SiO_2 insulator layer between the gate and the doped regions of the transistor, and the field oxide is much the same, save for its location, which is the area between transistors in the device (the edges of the transistor). All of the trapped charges themselves can be attributed to radiative effects resulting from compton scattering or similar. According to the study performed by SMU however, edge leakage current from accumulated charge in the field oxide has no effect on this particular SOS device by design, and thus is not the cause of the leakage current and threshold voltage changes[6]. The argument against the gate oxide contributing to the leakage current, versus the sapphire substrate, is one of size. The gate oxide is $6nm$ thick, while the sapphire substrate is $200micron$ thick. It is the conclusion of the study that the leakage current and threshold voltage changes must be attributed to trapped charge accumulations in the sapphire substrate[6]. Concerning the grounded sapphire substrate effects, other potentials other than ground level are applied in an ongoing study to better understand the mechanism by which the aforementioned radiative effects are mitigated[6]. As trapped charges are deemed responsible for leakage current and threshold voltage effects, a look at how radiation induced free charge migrates and behaves under an applied potential would be worthwhile in understanding the possible causes for such mechanisms. It is this purpose which drives an attempt at modeling free charge migration in Geant4 under the application of an electric field in sapphire, described in detail in chapter 3.

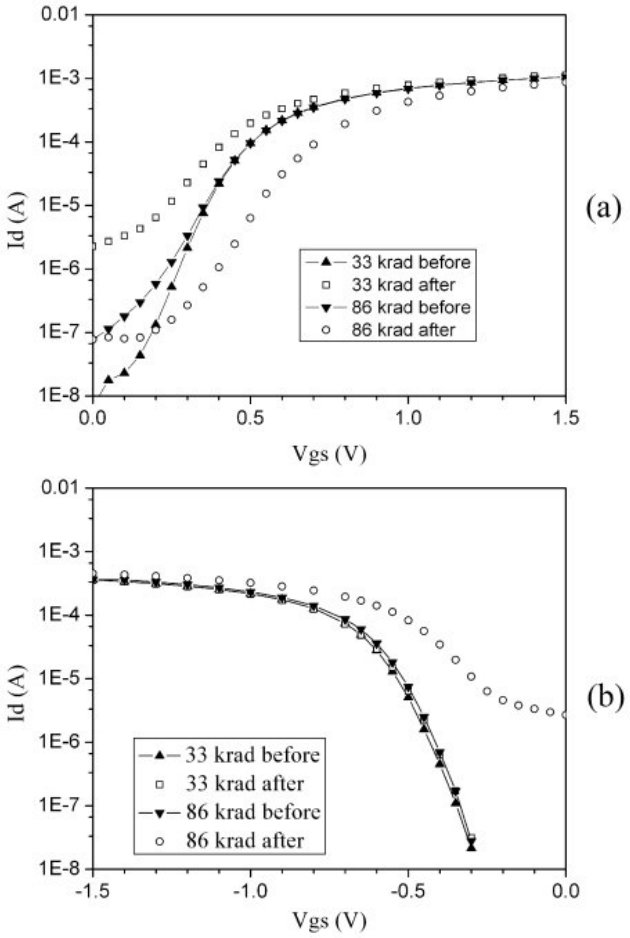

Figure 2.1. I-V curves, NMOS (a), PMOS (b)

2.3. Irradiated Sapphire, SEU

The very same device was subject to a single event upset (SEU) study done using a $230MV$ proton beam with normal incidence on the device. This is done as per the ATLAS specifications for single event effect (SEE) measurement[3]. An SEU is a phenomenon wherein a large amount of ionization in the device layer causes a single transistor device to switch digital states, resulting in bit flip. This is a sudden onset effect resulting from one single event (hence single event upset). A more in depth description of SEUs and other SEEs is beyond the scope of this document. The test parameters for SEU characterization involved a proton fluence of $1.8 \times 10^{12} protons * cm^{-2}$,

with a flux of $7.7 \times 10^8 protons * cm^{-2} * s^{-1}$. The test was done using a pseudo random bit stream passing input into the shift registers of the device, during irradiation. The output of the device is then compared to the input in a search for errors[6]. In this study, no errors was seen before, during or after the irradiation period. This imposes an cross section upper limit for SEU events of $5.6 \times 10^{-13} cm^2$ for all SEU test runs done[6]. An important question raised by this study is whether or not a change in orientation of the device would affect the SEU rate. The reason behind this is that the proton beam is directionally homogeneous and as such difference incidence conditions would result in different material exposure with respect to the device. The theoretical affects of changing the device orientation are explored in chapter 3 as another Geant4 based Monte Carlo study.

2.4. Sapphire Resistivity Experiment

As described in the Device section of this chapter, SOS devices are known to be radiation tolerant due to the high resistivity of artificially grown sapphire crystals. In an effort to track down the mechanism by which TID effects are suppressed while grounding the sapphire substrate, a study was done to measure the resistivity of the sapphire substrate during a similar TID radiation environment. Cobalt-60 is used as before for the irradiation. The test was done by applying a potential of 30 volts and measuring the current flow between 9 devices wired in parallel using a picoammeter. The resistivity was calculated using $R = V/I * A/L$ where A is the cross-sectional area of the device, and L is the path length along which the resistivity is measured. Since there are 9 devices in parallel, $L = 0.02cm$ and $A = 9 \times 0.3cm \times 0.30cm = 0.81cm^2$[3]. Shown in figure table 2.1 is the raw data from current measurements taken before and after the start of irradiation, and before and after the end of irradiation. Included in table 2.1 is also the calculated resistivities corresponding to the measured currents. As shown in table 2.1, current before irradiation is about $-3nA$ and immedietly after the start of irradiation, this current becomes positive. Likewise, current flow is positive right before the end of irradiation, but returns to about $-3nA$ after the end of irradiation. Shown in figure 2.3 is the continuously measured current as a function of time, throughout the irradiation process. Drastic changes can be seen in the areas corresponding to the start and end of irradiation. Figure 2.4 is a closer look at both the current versus time at the beginning and end of the irradiation process. It is clear from these figures that TID irradiation of the sapphire substrate creates a sudden change of resistivity. Although this result does not offer definitive explanations for the mechanism by which charge buildup could occur in the sapphire substrate during TID irradiation, it is clear that sapphire

Table 2.1. Current Measurements and Corresponding Resistivity Calculations

	$\boldsymbol{Current(A)}$	$\boldsymbol{Resistivity(ohm * cm^{-2})}$
before irradiation starts	-3.41×10^{-09}	-3.56×10^{11}
after irradiation starts	5.00×10^{-11}	2.43×10^{13}
before radiation stops	2.00×10^{-09}	6.08×10^{11}
after irradiation stops	-3.00×10^{-09}	-4.05×10^{11}

responds to irradiation and is susceptible to the affects therein.

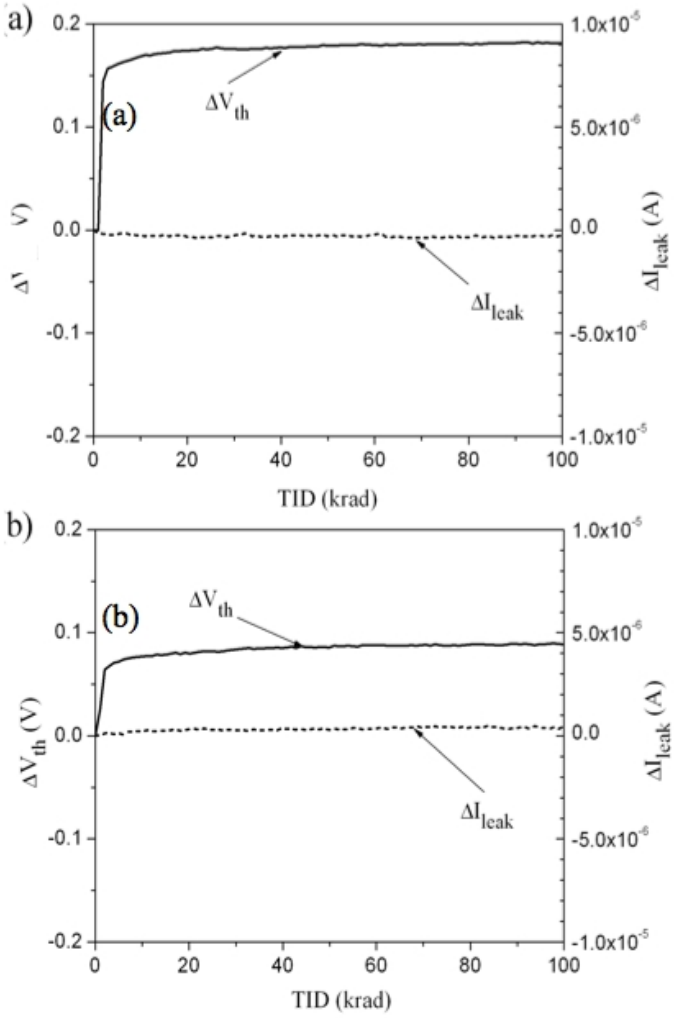

Figure 2.2. I-V curves, grounded substrate, NMOS (a), PMOS(b)

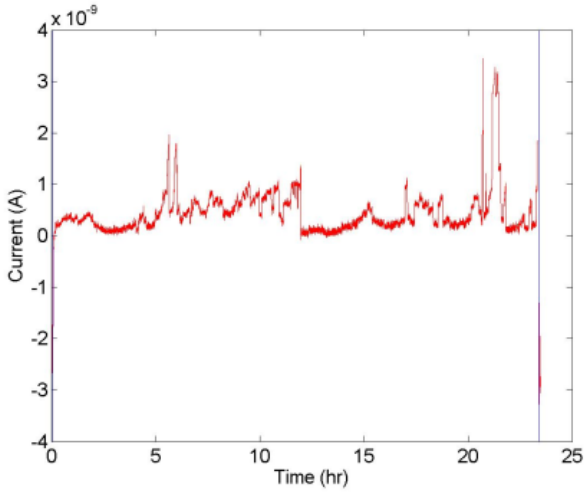

Figure 2.3. Current vs. Time

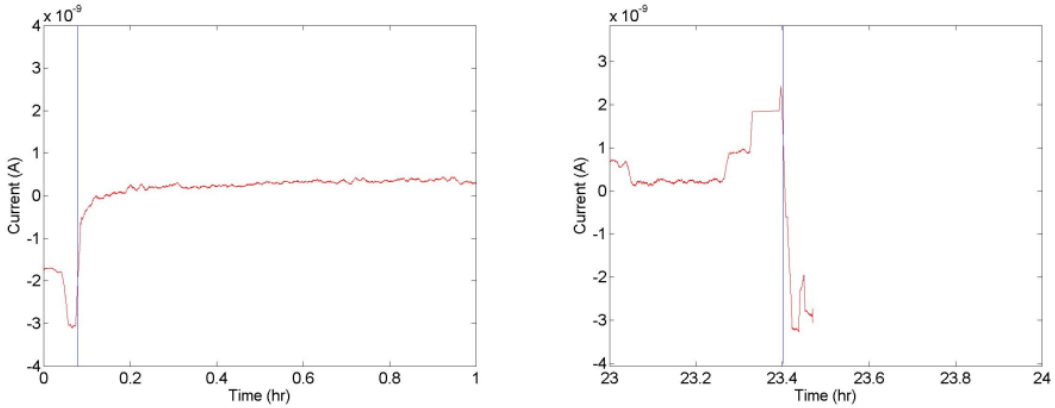

Figure 2.4. Current vs. Time, beginning and end

Chapter 3

MONTE CARLO STUDIES

3.1. Introduction

A series of Geant4 based Monte Carlo programs are run in an effort to better understand the physical sources of radiation induced behavior in the previously described semiconductor irradiation tests. The geometry used in the simulations is a simplified form of the physical experiments conducted by SMU. They are simplified in an effort to better understand the Geant4 toolkit in the process. The simulations are split into three major categories: protons incident on a series of printed circuit boards, simultaneous proton irradiation of silicon and sapphire blocks, and gamma irradiation of a single sapphire block with and without a uniform electric field.

3.2. Incident Proton Beam Divergence

3.2.1. Setup

As mentioned before, the setup for this simulation is a series of 10, equally spaced, Printed Circuit Boards (PCBs). The PCBs are composed of a material called FR4, or flame retardent #4. The thickness of each PCB is 0.062 inches, or 1.57mm. On the front side (the side facing against the proton beam) of each PCB is a 0.014 inch layer of copper (0.05mm). This is done to simulate the presence of copper eching used for the actual circuitry. The thickness is a result of common specifications used by many manufacturers of PCBs. Shown in figure 3.1 is the 3D visualization as produced by the Geant4 libraries. As can be seen the experiment area is defined as a box, $200mm$ cubed. At the center of this box is the origin, as well as the location of the first PCB. The rest of the PCBs are oriented along the positive z axis thereafter. Figure 3.1 illustrates an example of 20 proton interactions, some of which produce secondary particles. Positively charged particles have blue tracks, negatively charged particles have red tracks, and neutral particles have green tracks.

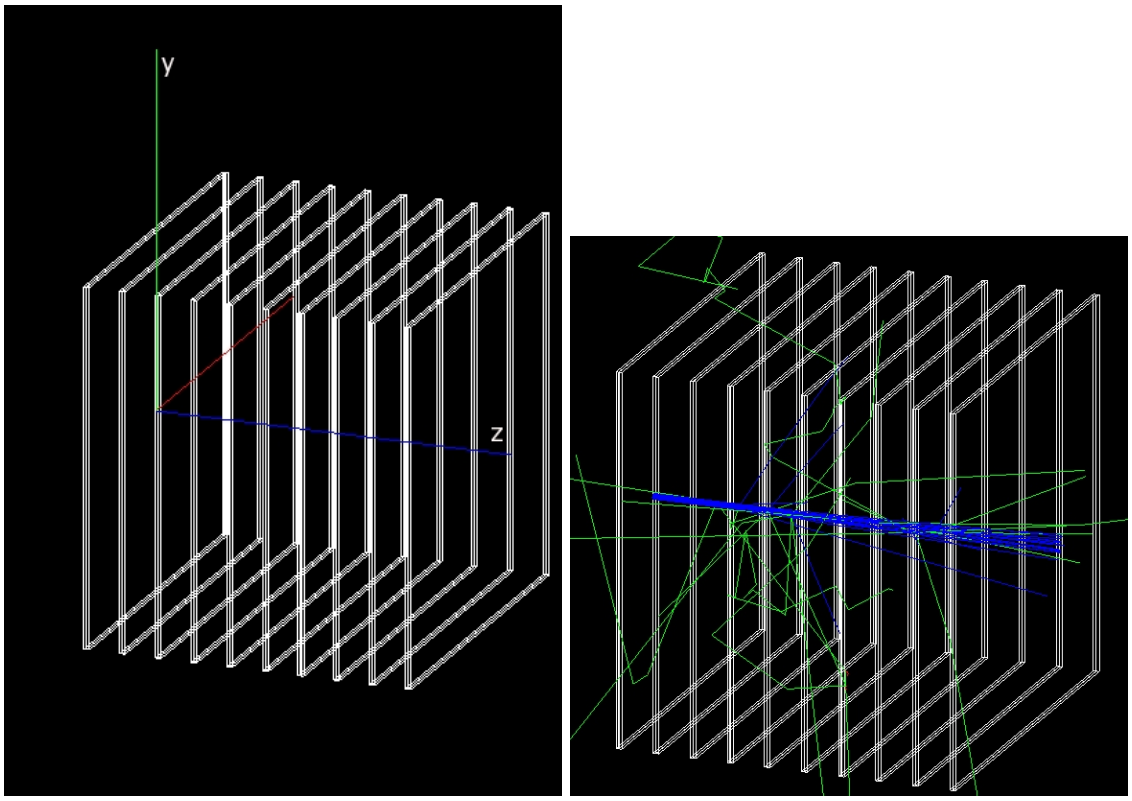

Figure 3.1. PCB Visualization geometry(left) and 20 event composite (right). positive charge particles in blue, neutral in green, and negative in red

Table 3.1. FR4 composition

Epoxy	*Percent*	***GlassFiber***	*Percent*	***FR4***	*Percent*
O	7.8	SiO_2	81.0	Epoxy	44.0
C	46.1	Na_2O	6.0	Glass	56.0
H	46.1	B_2O_3	13.0	***Density***	$1.9 * g/cm^3$

3.2.2. FR4 Material Description

As it is the crux of a Geant4 simulation, the composition of objects simulated is of great importance. FR4 is a glass-epoxy mixture used for it's self extinuishing charactersitcs. It is an industry standard material used in most applications where the spread of fire in electronics is not desired. The composition of FR4 as used in the simulation can be seen in table 3.1.

3.2.3. Beam Divergence Results

Shown in Figure 3.2 is the beam contour as it passes through the 1^{st}, 3^{rd}, 6^{th}, and 10^{th} PCB. As is clearly shown, the beam widens considerably as it passes through the boards. The number of entries between each image also hints at the loss of particles as the beam traverses the boards. These histograms where created by noting the x and y coordinates of each interaction in each PCB (and related copper layer). A "window" of z values is used to represent the qualifications for interactions in a certain PCB. This window is $2.0mm$ wide, and so for example interactions in the second PCB occur between $z = 9mm$ and $z = 11mm$, not inclusive. $2.0mm$ was chosen because the resulting histograms have a bin size of $0.5mm$ ($0.5mm$ square in 2D histograms), and so the precision is limited such that the $1.62mm$ cumulative width of each PCB looks like $2.0mm$. From 3.2, it is evident that by the 10^{th} PCB, any device lying on the face of the PCB will experience a different radiative environment than that of the 1^{st} PCB and, although the dominant incident particle at the 10^{th} PCB is still a $230MeV$ proton, secondary particles are plentiful. It is important to note that this simulation was done using only FR4 and copper, however a typical PCB is fully loaded with many components, ranging from microprocessors to capacitors. Some of these components, although small, have some very dense materials (such as the iron core of an inductor) which could produce a multitude of secondary particles.

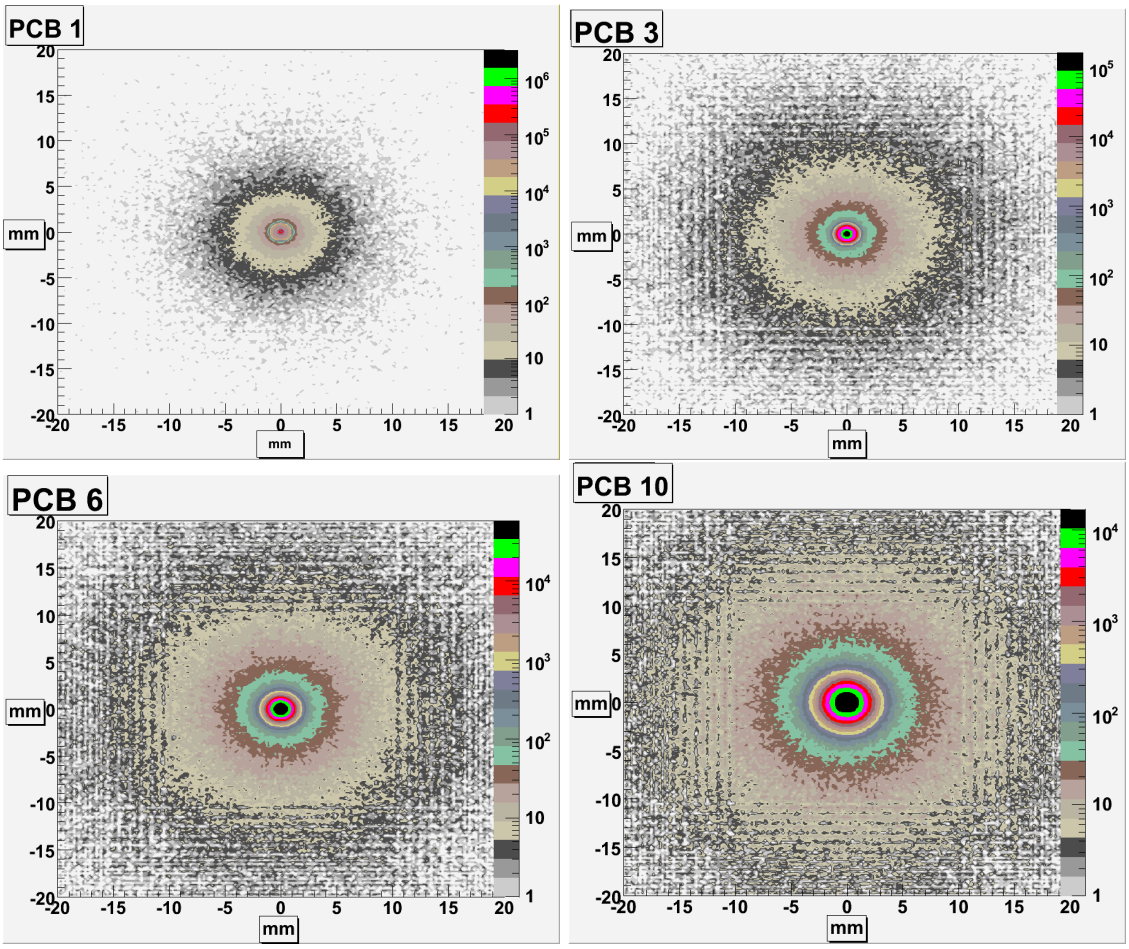

Figure 3.2. Beam Contour at PCB

Figure 3.3 is a look at the beam radius (that is, each proton interaction distance from the beam line) as the beam travels down the entire experiment. Particle data darken at each PCB due to there being a smaller step size resulting from a smaller mean free path. This behavior comes from Geant4 and the the fact that, step lengths of particles are based on their calculated mean free path in whatever the surrounding material is, and the global "cut" length imposed by the user. The width of the dark bands is not representative of the width of the PCB boards as this is a histogram. To clarify, the darker bands do not imply a sudden increase in interaction radius, but instead a sudden increase in data. Figure 3.3 is composed of each separate interaction wherein energy was lost. Each interaction position, as given in cartesian coordinates, is then used to calculate the distance of said

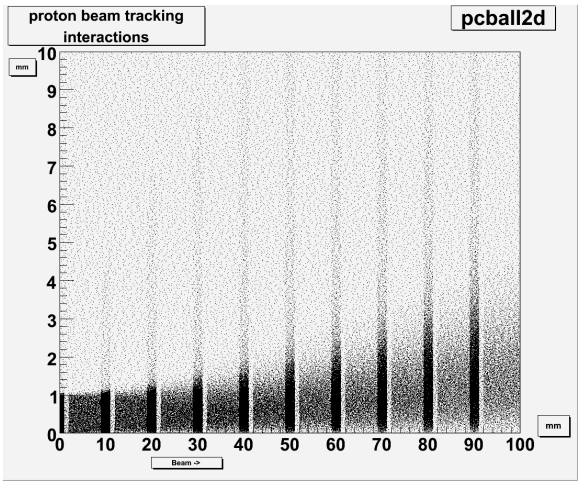

Figure 3.3. Proton Interaction Distance(mm) from Beam Center vs. Distance(mm) alont Beamline

interaction from the beam line. Figure 3.3 was the first attempt at visualizing the entirety of the experiment in one plot. Figure 3.3 characterizes the incident beam as it travels through the PCBs, and is consistent with the dispersion behavior seen in 3.2.

Figure 3.4 is an attempt to visualize how the dose drops towards the boundries of the experiment area. What is seen is a projection of all particle interactions and stepping events (as in, the particle is here but nothing happened), onto the $y - z$ plane. As expected, the first PCB (which is near $z = 0mm$) receives the highest dose, and the dose tappers off thereafter along the z axis. What is worth noting, is that the particle flux towards the top and bottom of the experiment area (near $y = 80mm$ and $y = -80mm$) is already less than 1% of the total particle count (as estimated from the contour palette shown). This can be related to the expected real-world time-dependent flux that would be seen in those areas. The right plot in figure 3.4 is the same particle interaction and tracking data from the left hand plot, projected once again to just the y axis, and plotted from the origin, to one end of the experiment, at $y = 100mm$.

3.2.4. Conclusions

A large concern of the experiments detailed in chapter 2 is that of ambient area contamination. Although experimental support digital electronics such as ammeters are shielded as best as possible, they still lie near the experiment area. Given these results, it seem reasonable to argue that little

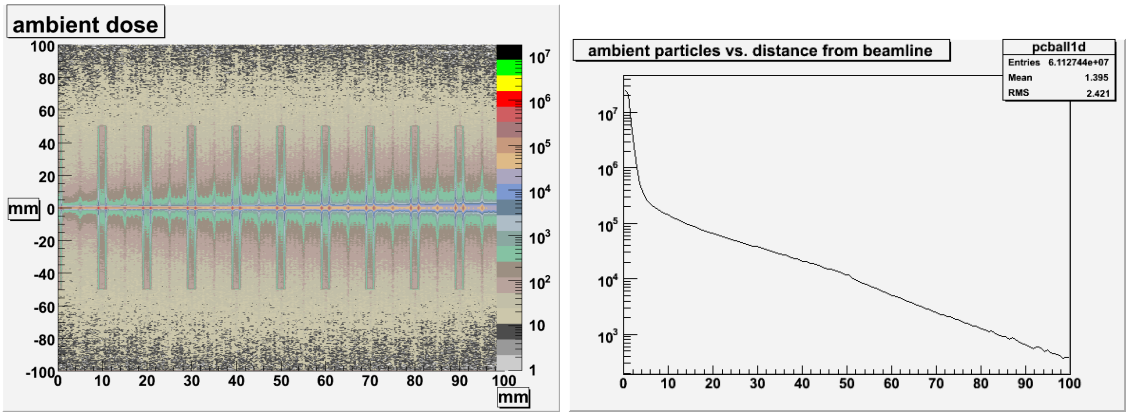

Figure 3.4. Ambient dose projection on to y-z plane (left) and further projection onto one quadrant of y plane

danger is posed to neighboring instruments. Since particle activity near the edges of the experiment is less than 1% that of initial beam activity, there is a minimal chance that electronic instruments used in any measurements would be affected by stray radiation. There is, however, a question as to how a Single Event Upset study changes as the incident beam becomes less focused, and increasingly heterogeneous from secondary particles. It at least has the effect of relaxing the imposed experimental control of $230MeV$ protons, which certainly brings the quality of such a study into question as more layers of electronics are stacked near each other for the purpose of irradiating multiple devices at once.

3.3. Silicon On Sapphire Proton Irradiation

In an effort to see the most probable cause for large scale upsets in the silicon layer (device layer), a crude model of a SOS device is created using a $100nm$ layer of silicon on top of a $200micron$ layer of sapphire. $230MeV$ protons are then shot at the silicon layer at normal, 30 and 60 degrees incidence and the same situation with the device orientation reversed (backwards). Close attention is given to produced ions, as they ionize heavily and subsequently produce a lot of damage. First, as shown in figure 3.5, the amount of interactions (wherein energy was deposited) is ploted versus the depth of the silicon layer. The silicon layer exists between $z = -100nm$ and $z = 0$, which is why the bottom scale of figure 3.5 starts at $-0.1e^{-03}mm$. Clearly the amount of interactions seen by the silicon

layer increases as the incident angle increases. Shown in figure 3.6 is the energy deposition spectra of interactions occuring in the silicon layer (the very same interactions depicted in figure 3.5). As expected, all of the curves in 3.6 have the same shape, however the integral of each curve increases with incidence angle, consistent with 3.5. From these two plots, it is reasonable to expect a larger single event upset (SEU) rate with a larger incidence angle. In other words, for proton radiation in a homogeneous direction, the orientation of a SOS device will affect the expected SEU rate, as it most certainly affects the energy deposition in the silicon layer.

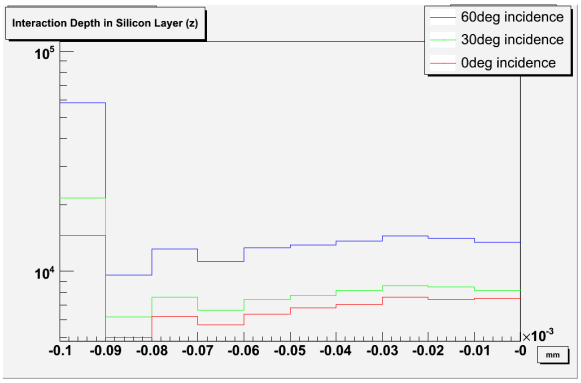

Figure 3.5. Interactions in Silicon Layer

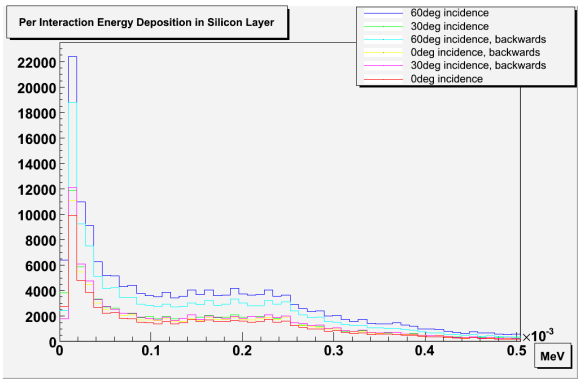

Figure 3.6. Energy deposition spectra in Silicon Layer

As promised, close attention is placed on heavy ion behavior. These ions come from nuclear interactions of the protons with silicon and sapphire. Since it is known that heavy ions do much

damage, it is also important to see what their lifetime (measured by their tracklength) is. Figure 3.7 shows the light and heavy ion ionization (measured by their energy deposition per length). This can best be described as the amount of damage these particles can do. This, coupled with figure 3.8, which shows ion lifetime (tracklength in mm), can give a better idea of if, logically, a change in orientation would effect the damage done by heavy ions.

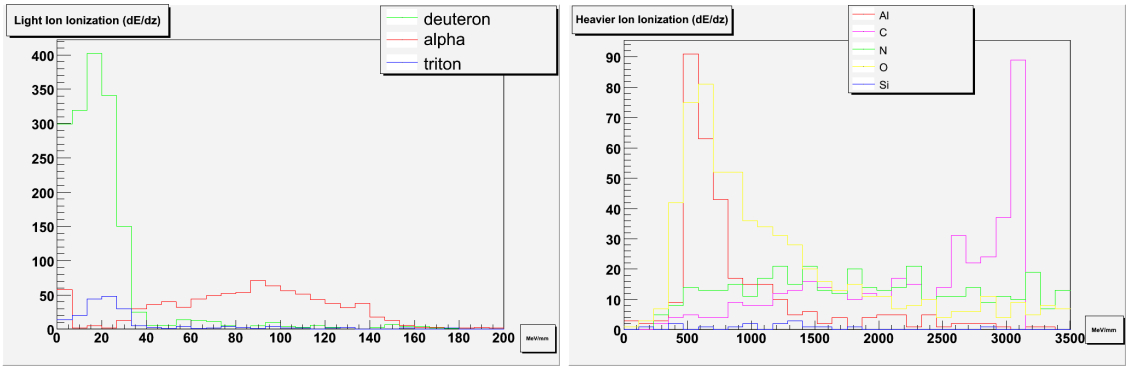

Figure 3.7. Ion Ionization in MeV/mm

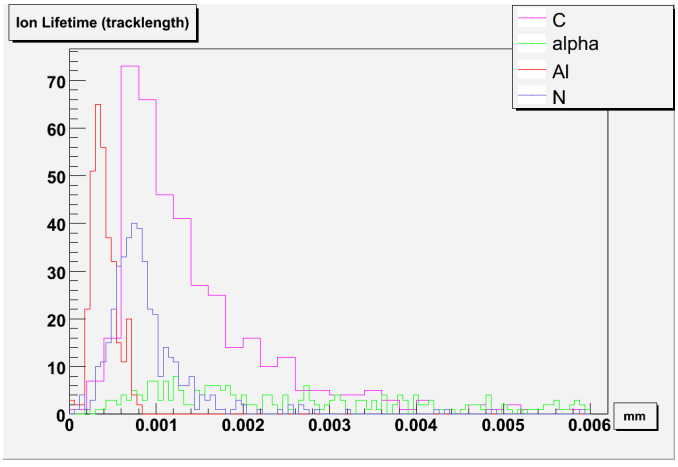

Figure 3.8. Ion Track Length in mm

3.3.1. Conclusions

From figure 3.8, it is clear that the path length of most heavy ions is greater than the width of the silicon layer, and as such, the total ionization should be affected by track angle with respect to normal incidence. Since ion track angles are biased by incident proton track angles, a greater incidence proton angle, will yield the same for ions, and thus greater possibility for energy deposition in the silicon layer. However, the most probably path length for ions (again from figure 3.8) is clearly much smaller than the sapphire layer depth, and as such any deviation from normal incidence will not effect the energy deposition from ions originating towards the back end of the sapphire layer. It is only interactions near the silicon layer that will actually reach the silicon layer. As SEU effects can be attributed, in large part, to released ions, a strong argument can be made, once again, for the increase in expected SEU rates from an increase in the proton incidence angle on the silicon layer.

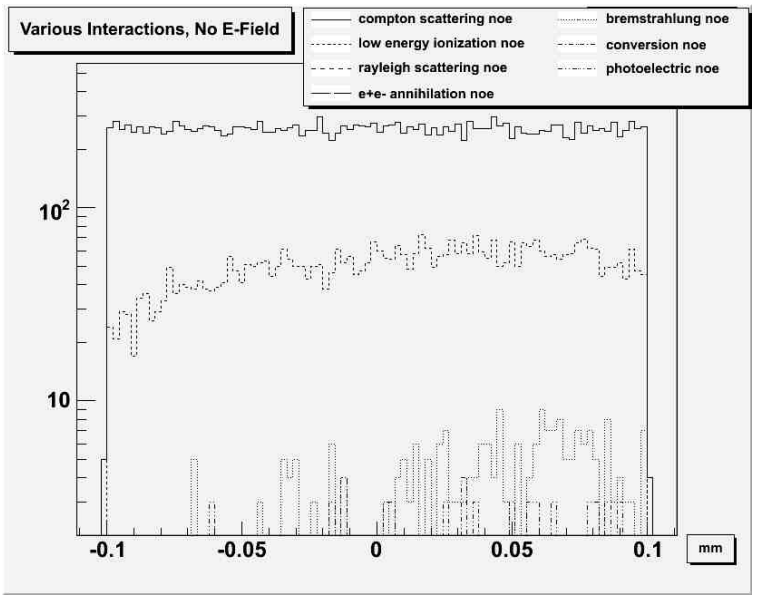

Figure 3.9. Various Interaction Types vs. Depth in Sapphire (mm), No E-Field

3.4. Sapphire Irradiation

In this simulation, as mentioned above, a 200 micron width sapphire block was irradiated with 1.2 MeV photons at normal incidence. The main goal is to see the resulting electron distribution under the influence of TID irradiation and an imposed electric field throughout the sapphire block. The electric fields used are $E = 150V * mm^{-1}$, $E = -150V * mm^{-1}$, $E = -1500V * mm^{-1}$, and no electric field. The large negative field is used to see if much change can be had by increasing the electric field to unreasonable levels. The choice of the other electric fields used corresponds to an applied potential $+30V$, $-30V$, and grounded. The resulting electrons (mostly from compton scattering as shown in figure 3.9) were then given close attention. As can be seen in figure 3.10, the distribution of trapped electrons is indeed affected by the various electric fields. This result suggests that and imposed electric field can affect the migration of electrons freed by TID radiation. This however does not give a complete picture of the effects of the electric fields on a SOS semiconductor device. As each electron produced leaves a positive charged "hole" in it's wake, this picture is not complete without a study of the behavior of these holes in the presence of an electric field.

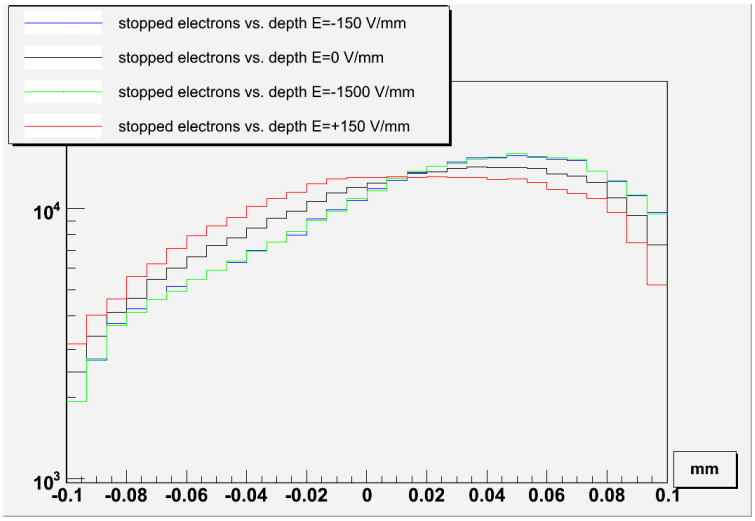

Figure 3.10. Stopped Electrons vs. Depth(mm) in Sapphire Block

Chapter 4

CONCLUSIONS

4.1. Geant4

In the previous Monte Carlo studies Geant4 was used exclusively. This low level use and understanding of Geant4, on this scale, is a first for SMU. The techniques involved include the compilation, modification, and use of the extensive Geant4 libraries, as well as optional features including various visualization interfaces, and the geometry definition frame work known as GDML[1]. The largest contribution is the knowledge of Geant4 which has been, with great effort, documented in order to pass on a valuable and newly annexed member of the SMU research infrastructure. Shown throughout the appendices is a working version of the simulation used in the aforementioned studies. It is still a work in progress, but it promises to provide an extensible, reliable means of small scale simulation of radiation with energies levels similar to those seen in these studies.

4.2. Conclusion

A main concern with the physical experiments described in chapter 2, is that of completeness. The question of whether or not the orientation of the SOS device contributed or mitigated single event upsets cannot easily be answered by more tests, and hence the simulations. As described in chapter 3, there is indeed a correlation between incident angle of the proton beam, and the energy deposition in the silicon layer (the device layer). In addition, heavy ion lifetimes in SOS material, measured in total path length, are greater than the thickness of the silicon layer. This is significant because heavy ions are predominantly produced by nuclear interactions with the incident protons. As a result, ions produced in such collisions have a biased direction, which is dependent on the incident angle of the proton beam. It can be concluded, then, that the heavy ionization by ions in the silicon layer is more damaging as the incident proton beam angle increases. Both of the aforementioned results lead to a theoretical increase in single event upsets as a result of an increase in proton beam incidence angle.

Related to the single event upset study mentioned above, the question of proton beam divergence as it passes through a series of printed circuit boards offered evidence for a small ambient dose (1% of incident dose) towards the limits of the simulated experimental area, a $200 \times 200 \times 200 mm^3$ cube. However, the dispersion of the proton beam offered a much different environment for the last printed circuit board, from that of the first printed circuit board.

The question of whether or not an electric field applied throughout the the sapphire substrate of a SOS device can affect the distribution of free electrons caused by TID irradiation was answered. An imposed electric field on the order of $150V * mm^{-1}$ can indeed affect the position where free electrons are finally trapped by the sapphire substrate. This however did not offer a complete explanation of the effect seen by the TID irradiation study done by SMU in which changes in leakage current and threshold voltages where minimized by grounding the sapphire substrate. Similarly, the results of the TID and electric field study are part of an ongoing study involving the correlation between imposed electric fields in sapphire, and the resistivity change therein.

REFERENCES

[1] *Geometry Definition Markup Language*. http://gdml.web.cern.ch/GDML/.

[2] *Root Object Oriented Framework Manual*. http://root.cern.ch.

[3] Radiation qualification of the front-end electronics for the readout of the atlas liquid argon calorimeters. Tech. rep., CERN, 2008.

[4] CERN. *Geant4 Manual*. http://cern.ch/geant4.

[5] Dentan, M. Atlas policy on radiation tolerant electronics. Tech. rep., CERN, July 2000.

[6] et al, T. L. Total ionization dose effects and single-event effects studies of a 0.25 μm silicon-on-sapphire cmos technology. Tech. rep., Southern Methodist University, March 2008.

[7] Liu, T. Irradiation test of optical fibers and the resistivity of sapphire. Tech. rep., Southern Methodist University, 2008.